High-resolution optical dating of Late Holocene storm surge deposits – a showcase from Schokland (Noordoostpolder, the Netherlands)

van den Biggelaar, D. F.A.M.; Wallinga, J.; van Balen, R. T.; Kasse, C.; Troelstra, S.; Kluiving, S. J.

published in
Earth Surface Processes and Landforms
2019

DOI (link to publisher)
10.1002/esp.4542

document version
Publisher's PDF, also known as Version of record

EARTH SURFACE PROCESSES AND LANDFORMS
Earth Surf. Process. Landforms **44**, 886–899 (2019)

Published online 17 December 2018 in Wiley Online Library
(wileyonlinelibrary.com) DOI: 10.1002/esp.4542

High-resolution optical dating of Late Holocene storm surge deposits – a showcase from Schokland (Noordoostpolder, the Netherlands)

D.F.A.M. van den Biggelaar,[1,2*†] J. Wallinga,[3] R.T. van Balen,[4,5] C. Kasse,[4] S. Troelstra[4] and S.J. Kluiving[2,6,7]

[1] Faculty of Science, Vrije Universiteit Amsterdam, Institute for Geo- and Bioarchaeology, De Boelelaan 1085, 1081 HV Amsterdam, the Netherlands
[2] Faculty of Arts, Vrije Universiteit Amsterdam, Research institute for the heritage and history of the Cultural Landscape and Urban Environment (CLUE), De Boelelaan 1105, 1081 HV Amsterdam, The Netherlands
[3] Soil Geography and Landscape group & Netherlands Centre for Luminescence dating, Wageningen University, PO Box 47, 6700 AA Wageningen, the Netherlands
[4] Earth and Climate Cluster, Faculty of Science, Vrije Universiteit Amsterdam, De Boelelaan 1085, 1081 HV Amsterdam, the Netherlands
[5] TNO - Geological Survey of the Netherlands, Princetonlaan 6, 3584 CB Utrecht, the Netherlands
[6] Department of Archaeology, Ancient History of Mediterranean Studies and Near Eastern Studies, Faculty of Arts, Vrije Universiteit Amsterdam, De Boelelaan 1105, 1081 HV Amsterdam, the Netherlands
[7] Faculty of Natural Sciences, Division of Biological and Environmental Sciences, University of Stirling, FK9 4LA, Scotland, United Kingdom

Received 24 March 2018; Revised 29 October 2018; Accepted 1 November 2018

*Correspondence to: D.F.A.M. van den Biggelaar, Institute for Geo- and Bioarchaeology, Faculty of Science, Vrije Universiteit Amsterdam, De Boelelaan 1085, 1081 HV Amsterdam, the Netherlands. E-mail: don.vandenbiggelaar@gmail.com
†Present address: IDDS, 's Gravendijckseweg 37, 2201 CZ Noordwijk, the Netherlands.

ESPL
Earth Surface Processes and Landforms

ABSTRACT: Storm surges have a major impact on land use and human habitation in coastal regions. Our knowledge of this impact can be improved by correlating long-term historical storm records with sedimentary evidence of storm surges, but so far few studies have applied such an approach. Here we apply, for the first time, state-of-the-art optically stimulating luminescence (OSL) methods to obtain high-resolution age information on a sequence of Late Holocene storm surge deposits. By combining this chronological framework of storm surges with other reconstruction methods, we investigate the storm surge impact on the former island Schokland, located in a former inlet of the North Sea (central Netherlands).During the Late Holocene, Schokland transformed from a peat area that gradually inundated (~800 CE) via an island in a marginal marine environment (~1600 CE) to a land-locked island in the reclaimed Province of Flevoland (1942 CE). These transitions are recorded in the sediment archive of the island, consisting of silty clay with sandy intervals deposited during storm surges. A series of ten quartz OSL ages, obtained using best-practice methods to deal with incomplete resetting of the OSL signal and dose rate heterogeneity, reveal two periods of storm surge deposition, around 1600 CE and between 1742 and 1822 CE. Historical sources indicate that major storm surges hit Schokland during these periods. Laboratory analyses (thermogravimetry, grain-size, foraminifera, bivalves and ostracods) corroborates the existence of the two sets of storm surge deposits within the clay sequence. Our study sets a benchmark for obtaining robust depositional age constraints from storm surge sediments, and demonstrates the great potential of modern OSL methods to contribute to improved assessment of storm surge risk. © 2018 John Wiley & Sons, Ltd.

KEYWORDS: coastal flooding; OSL dating; poor bleaching; sediment analysis; Medieval and Modern period

Introduction

Storm surges have a major socioeconomic and environmental impact in coastal regions. This impact is reflected by disasters such as the 1953 CE flooding in the southern North Sea area, which resulted in over 2200 fatalities across the Netherlands, the United Kingdom and Belgium (Steers, 1953; Waverley, 1954; Rijkswaterstaat and KNMI, 1961; Gerritsen, 2005). For the Netherlands, the financial cost of this disaster was estimated at 1.5 billion Dutch guilders (~675 million euro), which corresponded at that time to 6% of the gross national product and 23% of the national budget (Klijn and De Grave, 2008). More recent examples of storm surge induced disasters are the 2005 CE flooding in New Orleans by Hurricane Katrina that caused over 1000 deaths and USD 40–50 billion in monetary losses (unadjusted 2006 CE dollars) (Kates *et al.*, 2006;

Rappaport, 2014) and the 2012 CE coastal surge by Hurricane Sandy in the northeastern part of the US, which resulted in more than 100 fatalities and approximately USD 50 billion in damages (unadjusted 2013 CE dollars) (Blake *et al.*, 2013; CDC, 2013). During storm events such as these, there is an increased risk of coastal flooding due to extreme water levels. The total water level during a storm is the combined effect of the mean sea level, normal astronomical tide and storm surge (Flather and Khandker, 1993). As sea-level rise is an important consequence of the predicted climate change for the 21st century (Church *et al.*, 2013), and sea-level rise is most likely accelerating (Haigh *et al.*, 2014), high water levels will occur more frequently during future storms. This will increase the intensity of coastal hazards in the 21st century. In addition, possible changes in flood frequency and magnitude related to future climatic conditions (Seneviratne *et al.*, 2012), would further enhance coastal flood impact. Furthermore, in the low-elevation coastal zone (LECZ), defined by McGranahan *et al.* (2007) as the coastal areas that are less than 10 m above sea level, population is estimated to grow to at least a billion by 2060 CE (Neumann *et al.*, 2015). This growth will further increase the already high socioeconomic and environmental vulnerability of coastal areas to flooding. Apart from natural conditions, the effectiveness of disaster management measures also influences flood impact in these areas. Failure of such measures can have devastating consequences, as is clearly illustrated by the coastal disasters induced by Hurricane Katrina in 2005 CE (Kates *et al.*, 2006), the 2010 CE storm Xynthia in France (Kolen *et al.*, 2010) and the 2017 CE hurricanes Harvey and Irma in the Caribbean and the US Gulf Coast (Peiffer, 2017; Wintour, 2017; Worland, 2017). Apart from improving disaster management protocols, decreasing the probability of flooding is another means to reduce flood risk in the LECZ. Although there are a number of studies where the frequency of extreme sea levels is estimated (Lowe *et al.*, 2010; Menéndez and Woodworth, 2010; Muis *et al.*, 2016), many of these studies use instrumental records of sea level as input data for modelling. The instrumental record of sea level change consists of tide gauge measurements dating back to ~1700 CE and satellite altimeter data sets that cover the period from 1993 CE to present-day (Church *et al.*, 2013). The period covered in the instrumental record is shorter than the return period of major storm events, thereby reducing the precision in modelling the surge level of those low-probability events under a changing climate (Van den Brink *et al.*, 2005). To improve flood risk estimates it is of utmost importance to extend our understanding of storm frequency and magnitude beyond the period of instrumental records (De Kraker, 2002; Buynevich *et al.*, 2007; Cunningham *et al.*, 2011a; Van Vliet-Lanoë *et al.*, 2014). Therefore, the timing of historical storm surges and their impact on coastal areas needs to be investigated.

One of the areas in the LECZ where storms had a major influence on the lives of its inhabitants was the former island Schokland in a former inlet of the North Sea (central Netherlands) (Figure 1(A) and (B)). The population at Schokland struggled against the impact of the North Sea for several

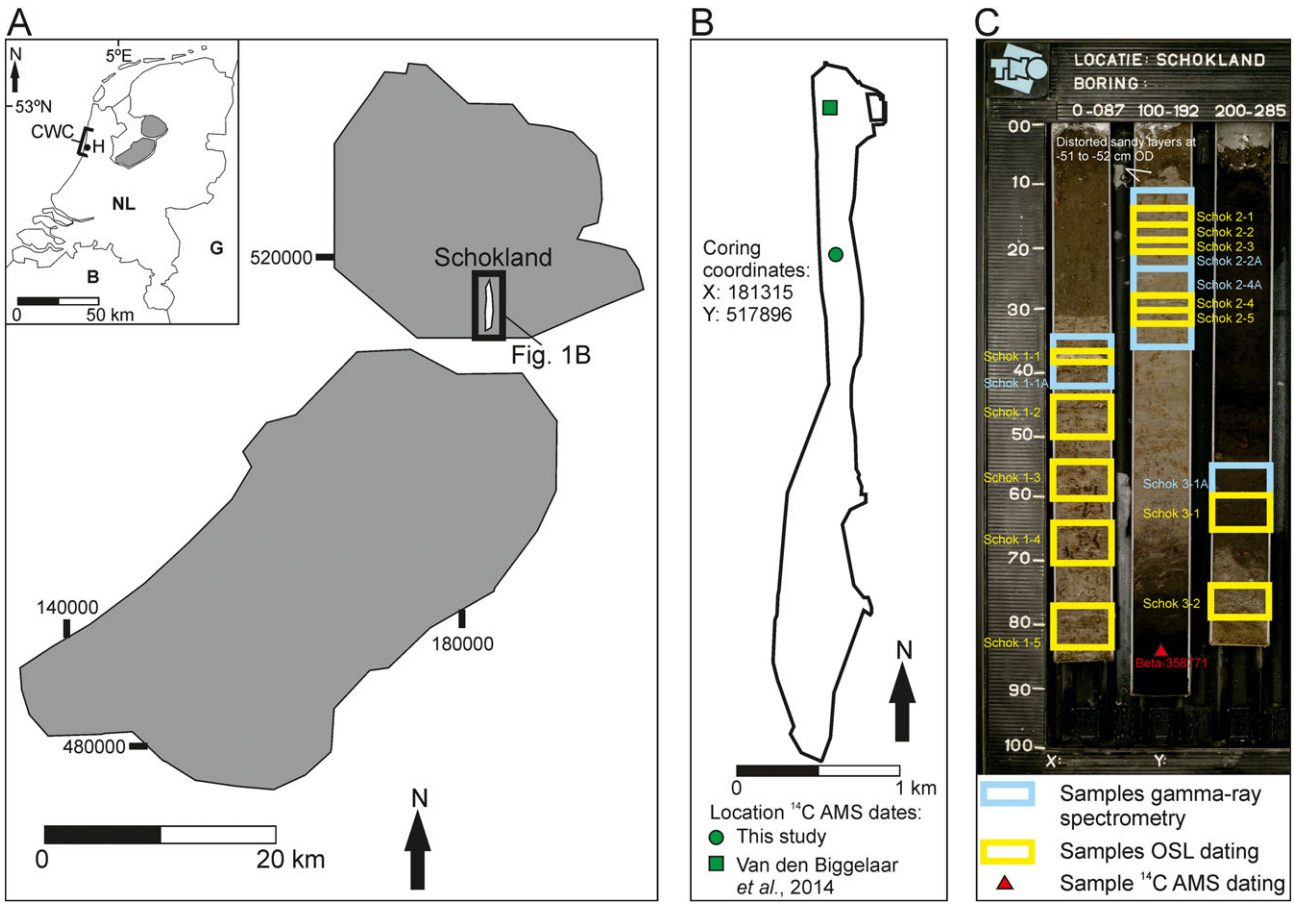

Figure 1. (A). Location of Schokland within the reclaimed area of Flevoland (grey area) and the Netherlands is shown, together with the areas where storm surge sediments were located that were investigated by Jelgersma *et al.* (1995; cwc – central western coast) and Cunningham *et al.* (2011a; H – Heemskerk). The map has a 'Rijksdriehoekstelsel' coordinate system (Dutch National coordinate system). (B) Location of coring and ^{14}C AMS dates (circle: this study; square: Van den Biggelaar *et al.*, 2014). Coordinates of the coring are in the Dutch National coordinate system. (C) Detailed view of the core and location of samples for OSL and AMS dating, together with the position of the distorted sandy layers at –51 to –52 cm OD (108 to 109 cm below the surface). The depth in cm below surface is plotted on the y-axis. [Colour figure can be viewed at wileyonlinelibrary.com]

centuries (Van den Biggelaar *et al.*, 2014), which ended after the evacuation of 1859 CE (Handelingen Staten-Generaal, 1858–1859 in Geurts, 1991). During the Late Holocene, Schokland transformed from a peat area that gradually inundated (~800 CE) (Ente *et al.*, 1986; Van den Biggelaar *et al.*, 2014) via an island in a marine environment (~1600 CE) to a land-locked 'island' in the reclaimed Province of Flevoland (1942 CE) (Van der Heide and Wiggers, 1954). A detailed overview of the island's depositional history during the last 1200 years is presented by Van den Biggelaar *et al.* (2014). Deposits formed on Schokland between 800 and 1942 CE, consist of silty clay and sand layers, with the latter being attributed to reworking of the Pleistocene subsurface by storm surges (Van den Biggelaar *et al.*, 2014). These sandy layers have been tentatively correlated to Late Holocene storm surges (Van den Biggelaar *et al.*, 2014), but their exact age is thus far unknown.

To improve flood risk assessment it is important to date storm surge sediments with a high degree of precision. There are a number of studies where optically stimulating luminescence (OSL) dating was used to date major storm surge events and investigate coastal response to these events (Buynevich *et al.*, 2007; Cunningham *et al.*, 2011a; Fruergaard *et al.*, 2013). Here we attempt, for the first time, to establish a high-resolution storm chronology through direct dating of a sequence of storm surge deposits. However, dating of storm surge sediments at Schokland by OSL is complicated by two factors. First, at the former island these sediments have thin intervals (2–20 mm: Van den Biggelaar *et al.*, 2014), making it challenging to extract sufficient material for dating. Second, flooding of large parts of Schokland during storm surges (Meijlink, 1858), combined with the deposition of reworked Pleistocene sands at the former island during those storms (Van den Biggelaar *et al.*, 2014), indicates that storm surge sediments were most likely deposited subaquatic together with large amounts of suspended material. Under these conditions, there is a high probability that these sediments were exposed to reduced ambient light levels during transport, inducing the risk of incomplete resetting of the OSL signal, which may result in overestimation of depositional ages. In order to establish a storm surge chronological record of Schokland, we combine for the first time a set of best-practice approaches to deal with methodological challenges posed by the thin flood deposits and difficult bleaching circumstances. Thereby we present a new benchmark for obtaining robust depositional age constraints from storm surge sediments that are both heterogeneous on a millimetre scale and exposed to limited amounts of light prior to burial.

To establish a geochronological framework, sandy laminae in the clay deposits are dated using ten OSL samples from sand deposits associated with storm surge events. To strengthen the age model for the basal part of the core, two additional OSL age determinations (sand material), and one ^{14}C accelerator mass spectrometry (AMS) dating (organic material) were made. The second objective of this research is to obtain insight to the events that lead to the abandonment of Schokland. For this purpose the core was analysed for thermogravimetric analysis (TGA), grain size analysis (GSA), foraminifera, bivalves and ostracods to reconstruct palaeoenvironments.

Site

Around 800 CE a tidal inlet in the northwestern part of the Netherlands opened (Vos and De Vries, 2013), advancing the connection between the North Sea and the Flevo lagoon that existed at that time in the centre of the Netherlands (Figure 2). Since the opening of this tidal inlet, storm events have had access to this lagoon, hereby transforming the area into an inlet of the North Sea that was called the Zuiderzee. It is assumed that

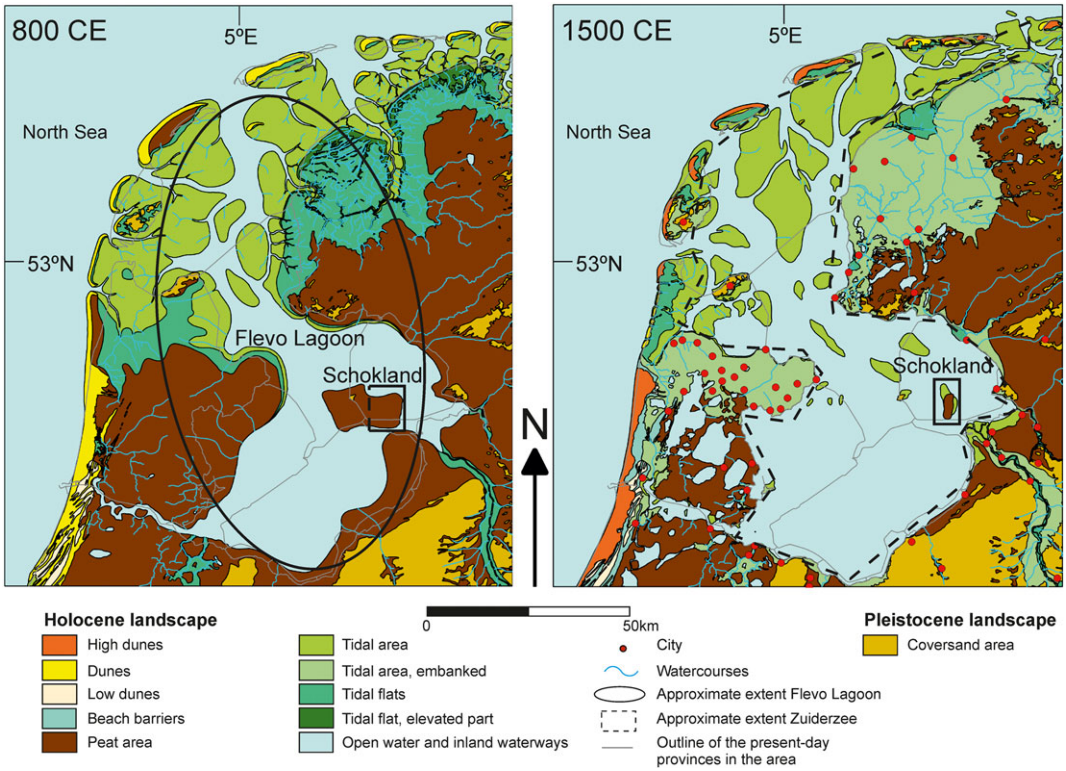

Figure 2. Palaeogeographical maps of the northwestern part of the Netherlands (modified after Vos and De Vries, 2013, adapted from Van den Biggelaar *et al.*, 2014), showing the approximate extent of the Flevo Lagoon in 800 CE, of the Zuiderzee in 1500 CE and of Schokland in both 800 and 1500 CE maps. The approximate size of Schokland in 800 CE is based on the study by Van der Heide and Wiggers (1954). The western extent of Schokland at 800 CE is unclear and therefore indicated by a dashed line. [Colour figure can be viewed at wileyonlinelibrary.com]

this transformation was completed by the storm event of 1248 CE (Buisman, 1995). For the inhabitants of Schokland the formation of the Zuiderzee initiated the struggle against the sea. This struggle started with the construction of embankments at the island around 1200 CE (Van der Heide and Wiggers, 1954; Hogestijn, 1992). Due to the increasing influence of the Zuiderzee in the area these embankments and their back-barrier zones were gradually lost to the sea, causing people to move to artificially raised areas (mounds) on Schokland halfway through the 15th century (Figure 3) (Van der Heide and Wiggers, 1954). Between the early 17th century and late 18th century the surface area of Schokland had shrunk to half of its original size due to the continued erosion by the Zuiderzee (Van der Heide and Wiggers, 1954; Figure 3), despite the presence of a wooden sea defence at that time along parts of the former island (Moerman and Reijers, 1925). To prevent any further loss of land by the Zuiderzee a stone embankment was built at the western coast of Schokland at the beginning of the 19th century (Moerman and Reijers, 1925). However, the storm surges of 1824 and 1825 CE caused heavy damage to this embankment and the former island (Moerman and Reijers, 1925), which led to the replacement of this embankment by a shore consolidated with stones (Mees, 1847). After the evacuation of Schokland in 1859 CE the area suffered most from the storm surges of 1877 (Van der Heide, 1963) and 1916 CE (Zuiderzee-vereeniging, 1916). After the 1916 CE storm surge a bill concerning the construction of the Zuiderzee works was accepted by parliament in 1918 CE (Van der Wal, 1923), leading to the reclamation of land now part of the (polders of the) Province of Flevoland around 1942 CE. Since that time, Schokland is a unique land-locked island, which has a UNESCO World Heritage status.

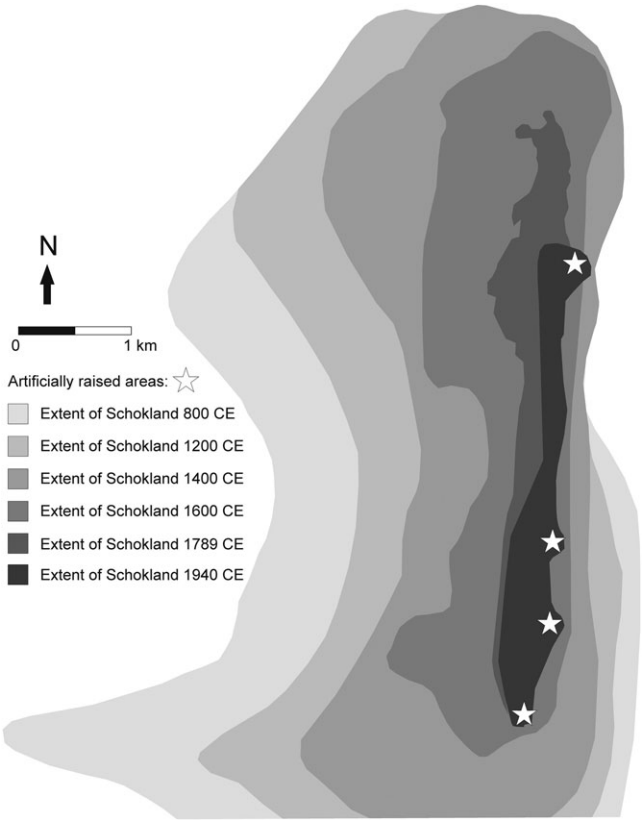

Figure 3. The loss of land at Schokland since 800 CE (after Wiggers, 1955, adapted from Van den Biggelaar *et al.*, 2014), together with the location of the artificially raised dwelling mounds that were inhabited since the 15th century (Van der Heide and Wiggers, 1954).

Storm surges not only caused erosion on the island fringes, but also brought new sediments, stacked up as storm deposits in more central parts of the island. The number of sandy laminae within the clay deposit that formed at Schokland between 800 and 1942 CE varies across the former island (Van den Biggelaar *et al.*, 2014). For this research the location with the highest number of these laminae was selected (compare Figure 10 in Van den Biggelaar *et al.*, 2014 and Figure 1(B) in this study).

Methods

Coring and sampling

A mechanical bailer-drill coring (10 cm diameter) (Oele *et al.*, 1983) was performed at Schokland by a team from Wiertsema & Partners BV (Figure 1(B) and (C)). The undisturbed cored samples were collected in three 1-m length light-tight PVC tubes. The location of the coring was measured with a GPS (accuracy < 1 m). At TNO Geological Survey of the Netherlands (TNO) the cored 1-m tubes were split longitudinally in two parts in a dark room under subdued amber light. One half was brought into ambient light, and used for the lithological description at TNO according to standard guidelines (Bosch, 2000). After description, this half was sampled at 10-cm intervals in the sedimentological lab of the Vrije Universiteit Amsterdam for GSA, TGA and palaeo-ecological indicators (foraminifera, bivalves and ostracods). In addition, the peat–clay transition was sampled at 1-cm intervals for TGA, and a 2-cm thick sample was taken from organic material for ^{14}C AMS dating of the top of the peat. From the other half, which remained in the dark room, we took 12 samples for OSL dating and four additional samples for gamma-ray spectrometry (see Figure 1(C)).

Grain size samples were pre-treated with H_2O_2 (30%) and HCl (10%) to remove organic matter and carbonate. To determine the grain size distribution of the samples (in vol%) a Helos KR Sympatec laser diffraction particle sizer was used. The organic matter and carbonate content of the samples (in weight %) was determined with a Leco 701 by stepwise heating from 25 to 1000°C.

C-14 dating

The terrestrial plant and seed material was manually selected from the ^{14}C AMS sample, to avoid contamination with younger or older carbon. At the Beta Analytic facility in Miami (US) the sample was then prepared for dating by using the AAA method of Mook and Streurman (1983). At this facility, the radiocarbon date was calibrated with the IntCal09 calibration curve (Reimer *et al.*, 2009), using the software developed by Talma and Vogel (1993). Following radiocarbon convention, the resulting age is given with a 95% (2-sigma) confidence interval. To facilitate comparison with OSL ages, calibrated ages are expressed in CE (Common Era), using the Gregorian calendar.

OSL dating: OSL dating analyses were performed at the Netherlands Centre for Luminescence dating (NCL), Wageningen University. To obtain an OSL age the amount of radiation received by the sample since the time of burial (palaeodose, Gy) is divided by the absorbed radiation amount per 1000 years (dose rate, Gy/ka). OSL dating for these type of deposits is not straightforward, due to the lithological heterogeneity, the relatively young age, and expected limited light exposure prior to deposition. A combination of methods was used to overcome these challenges. With regard to dose rate estimation, two methods were used in combination: First, gamma-ray spectrometry to determine radionuclide activity concentrations for

samples from larger intervals, and for relatively homogeneous intervals. Second, Instrumental Neutron Activation Analysis (INAA, performed at the Reactor Institute Delft, TU Delft) for determining elemental concentrations for sandy laminae from the heterogeneous parts. No radioactive disequilibrium was observed for any of the samples measured with gamma-ray spectrometry. For many samples (see Table I), dose rate contributions from different layers were combined to derive dose rate estimates for the sample prepared for palaeodose estimation, taking into account the penetration depth of beta particles (typically 1–2 mm) and gamma-rays (roughly 20 cm). A layer model was constructed towards this, to allow determination of the relative contribution of different layers, based on formulas provided in Aitken (1985), and using methods previously described in Wallinga and Bos (2010) and Cunningham *et al*. (2011b). Radionuclide activity concentrations (gamma spectrometry) and elemental concentrations (INAA) were converted to dose rates using the conversion factors of Guérin *et al*. (2011). Grain-size attenuation for beta particles was incorporated following Mejdahl (1979). Water and organic matter content were measured on the samples prepared for gamma-ray spectroscopy, and these estimates (Table I) are used for calculating attenuation factors (following Aitken, 1998). To account for variations over time, relatively large uncertainties of 25% were assumed for water and 10% for organic content estimates. For laminae of pure sand, a water content of 20 ± 5% was used based on a porosity of 34% and assuming full saturation during the period of burial. A full account of which input was used for each of the samples is provided in Table I. With respect to the contribution of cosmic rays, gradual burial of the deposits was assumed based on the geological setting (Van den Biggelaar *et al.*, 2014), and calculations were based on Prescott and Hutton (1994) and Madsen *et al*. (2005).

Sand-sized grains of quartz were prepared for OSL analysis. The 180–212 µm fraction was used in case this provided sufficient material. For other samples the 90–180 µm (NCL-7613040), 63–90 µm (NCL-7613041-45) or 212–250 µm (NCL-761346-47) fraction was used. For equivalent dose (D_e) estimation the Single Aliquot Regenerative (SAR) dose procedure was used (Murray and Wintle, 2003) using a pre-heat of 180°C or 200°C, in combination with a cutheat of 160°C or 180°C. To optimize the contribution of the most light-sensitive signal (fast component) to the OSL signal, an early background approach was adopted (Cunningham and Wallinga, 2010) using the OSL signal during the first 0.5 s of stimulation, minus that observed during the subsequent 1.25 s. The procedure was tested using a dose-recovery test, showing that measured radiation doses match closely with the given doses (dose recovery ratio is 0.97±0.06; n = 14 (pre-heat 180°C) and 0.99±0.03; n = 19 (pre-heat 200°C)). Equivalent dose measurements were made on small aliquots (1 mm diameter; yielding between 15 and 150 grains, depending on the grain size used for analysis). These small aliquots were used to obtain insight to grain-to-grain variations in D_e. The D_e distributions of the samples indicate overdispersion (Table II), which, based on the age and depositional environment, is most likely caused by heterogeneous bleaching. To avoid burial age overestimation due to heterogeneous bleaching the bootstrapped version of the Minimum Age Model (MAM; Galbraith *et al*., 1999; Cunningham and Wallinga, 2012) was used to estimate the palaeodose from the measured distribution. In the bootstrapped MAM (BSMAM), we assumed an overdispersion of 16 ± 4% for well-bleached deposits with sample grain size of 180–212 µm based on an analysis of observed overdispersion on the best-bleached samples. The overdispersion assumption was adjusted for other grain sizes (see Table 2) used for analysis as it depends on the number of grains contributing to the OSL signal of the aliquot (cf. Cunningham *et al*., 2011b, following the procedure outlined in Chamberlain *et al*. (in press)).

Following conventions in OSL dating, OSL ages are presented in ka (relative to year of sampling; 2012 CE) with errors indicating 68% (1-sigma) confidence interval. Presented uncertainties include both random and systematic errors. For comparison with radiocarbon ages and historical data, ages are expressed in CE (Common Era).

Sample summary

The laboratory sampling strategy yielded 34 TGA, 15 GSA, 16 palaeo-ecological, one AMS radiocarbon, 12 OSL (of which six were also used for INAA and five for gamma-ray spectrometry analyses), and four additional gamma-ray spectrometry samples.

Results

An overview of the lithology and corresponding GSA, TGA, palaeo-ecological indicators, ^{14}C AMS date and OSL dating results is shown in Figure 4. Detailed information on the dating results is given in Table II (OSL) and Table III (^{14}C AMS).

Lithology

Based on lithological characteristics, the core can be divided into three units. Unit 1, located at the base of the core (below –203 cm Dutch Ordnance Datum (OD, ~mean sea level)), consists of slightly and medium silty sand that is light to dark brownish grey. Unit 2 (–203 to –123 cm OD) consists of dark brown mineral-poor reed or sedge peat with a total thickness of 80 cm. The peat is covered by unit 3 (–123 to 57 cm OD), a clay sequence with a thickness of 180 cm that consists of light brown–grey medium to very silty clay. This clay sequence contains the thin sandy layers which have been dated by OSL. Overall, the sand and $CaCO_3$ content in the clay sequence increases towards the top and the organic matter content decreases (Figure 4).

Palaeo-ecological indicators

The upper part of the reed and sedge peat sequence of unit 2 (–128 to –126 cm OD) contains seeds from *Galium palustre* and *Epilobium*, implying that the area was located within a reed-sedge swamp at the time of formation. The basal 20 cm of the clay sequence (–123 to –103 cm OD) (unit 3) contains abundant *in situ* plant remains, relatively low $CaCO_3$ content (max. ~4.7 wt%) and the arenaceous foraminifer *Trochammina* sp. (Figure 4). This foraminifer species is indicative of occasional saltwater inundation (e.g. during spring tide) and is commonly found in mudflats (Murray, 2006). Seeds of *Ranunculus* are also present, which, combined with the presence of agglutinated foraminifera (*Trochammina* sp.), indicate weakly brackish conditions. The overlying 80 cm of clay (–103 to –23 cm OD) contains few calcareous foraminifers (e.g. *Ammonia beccarii*). The presence of *Ammonia beccarii* indicate a salinity between ~10 and 31‰ (Murray, 2006), implying that they can occur in brackish to marginal marine conditions. The upper part of the clay deposit (top 80 cm, –23 to 57 cm OD) contains bivalve shell material, ostracods and the calcareous foraminifer species *Ammonia beccarii* and *Haynesina* sp. The presence of both *Ammonia* and *Haynesina* indicate a salinity of at least

Table I. Results of the INAA and gamma-ray spectroscopy (GS). Also, the texture of the sampled material, thickness of the sampled sandy layers and the water and organic matter content (weight %, relative to dry sediment weight) used for beta and gamma dose rate estimation is shown. For the samples NCL-7613037–40 the thickness of the sampled sandy layers could not be determined due to the heterogeneous texture of the sampled interval

NCL code	Sample code	Depth sample (m below surface)	Elevation sample (m Dutch O.D.)	Texture	Thickness of sampled sandy layer (mm)	INAA elemental concentration (mg/kg)			Gammaspec activity concentration (Bq/kg)*			Water content (% dry weight)		Organic matter content (% dry weight)		Method used for dose rate estimation****	
						K	U	Th	K-40	U-238*	Th-232**	Measured	Used***	Measured	Used***	Beta dose rate	Gamma dose rate
NCL-7613036	Schok 1-1	0.37-0.39	0.18-0.20	slightly silty medium fine sand	20	7700 ± 539	0.56 ± 0.07	2.39 ± 0.10					20 ± 5		3.0 ± 1.0	INAA sample	Layer model INAA sample & GS NCL-7613048
NCL-7613037	Schok 1-2	0.44-0.50	0.07-0.13	very silty clay with lenses and layers of loam and sand	not available (bulk sample)				497 ± 15	32.9 ± 0.5	37.4 ± 1.0	28	28 ± 7	3.2	3.2 ± 0.3	GS sample	Layer model GS (NCL-7613037, 38,48)
NCL-7613038	Schok 1-3	0.54-0.60	-0.03-0.03	very silty clay with lenses and layers of loam and sand	not available (bulk sample)				445 ± 13	31.2 ± 0.5	32.7 ± 0.9	27	27 ± 7	3.7	3.7 ± 0.4	GS sample	Layer model GS (NCL-7613037-39)
NCL-7613039	Schok 1-4	0.64-0.70	-0.13 - -0.07	very silty clay with lenses and layers of loam and sand	not available (bulk sample)				527 ± 12	29.8 ± 0.5	38.2 ± 1.1	31	31 ± 8	2.6	2.6 ± 0.3	GS sample	Layer model GS (NCL-7613038-40)
NCL-7613040	Schok 1-5	0.77-0.83	-0.26 - -0.20	very silty clay with lenses and layers of loam and sand	not available (bulk sample)				578 ± 13	32.7 ± 0.5	41.1 ± 1.2	36	36 ± 9	3.1	3.1 ± 0.3	GS sample	GS sample
NCL-7613041	Schok 2-1	1.14-1.16	-0.59 - -0.57	very silty clay with sandy layer	4	18800 ± 940	2.3 ± 0.2	10.1 ± 0.5					45 ± 11		4.7 ± 0.5	INAA sample	GS (NCL-7613049)
NCL-7613042	Schok 2-2	1.16-1.18	-0.61 - -0.59	very silty clay with sandy layer	2	20000 ± 1600	2.5 ± 0.2	10.9 ± 0.3					45 ± 11		4.7 ± 0.5	INAA sample	GS (NCL-7613049)
NCL-7613043	Schok 2-3	1.18-1.20	-0.63 - -0.61	very silty clay with sandy layer	3	20001 ± 1600	2.7 ± 0.2	10.6 ± 0.4					45 ± 11		4.7 ± 0.5	INAA sample	GS (NCL-7613049)
NCL-7613044	Schok 2-4	1.28-1.30	-0.73 - -0.71	very silty clay with sandy layer	5	20002 ± 1600	2.2 ± 0.2	10.9 ± 0.3					44 ± 11		4.1 ± 0.4	INAA sample	GS (NCL-7613050)
NCL-7613045	Schok 2-5	1.30-1.32	-0.75 - -0.73	very silty clay with sandy layer	1	18700 ± 748	2.3 ± 0.2	11.0 ± 0.3					44 ± 11		4.1 ± 0.4	INAA sample	GS (NCL-7613050)
NCL-7613046	Schok 3-1	2.60-2.66	-2.09 - -2.03	medium silty very fine sand	60											GS avg. (NCL-7613047,51)	Layer model GS (NCL-7613047, 51) and peat attenuation
NCL-7613047	Schok 3-2	2.74-2.79	-2.22 - -2.17	slightly silty very fine sand	50				298 ± 9	12.0 ± 0.2	10.9 ± 0.4	14	20 ± 5	0.8	0.8 ± 0.1	GS sample	GS sample
NCL-7613048	Schok 1-1A	0.34-0.42	0.15-0.23	very silty clay with interval of slightly silty medium fine sand	not applicable				453 ± 11	27.2 ± 0.5	29.4 ± 1.0	25	25 ± 6	2.2	2.2 ± 0.2	n.a.	n.a.
NCL-7613049	Schok 2-2A	1.11-1.23	-0.66 - -0.54	very silty clay	not applicable				689 ± 15	38.9 ± 0.6	48.4 ± 1.3	45	45 ± 11	4.7	4.7 ± 0.5	n.a.	n.a.
NCL-7613050	Schok 2-4A	1.23-1.36	-0.79 - -0.66	medium to very silty clay	not applicable				728 ± 16	39.9 ± 0.6	49.1 ± 1.3	44	44 ± 11	4.1	4.1 ± 0.4	n.a.	n.a.
NCL-7613051	Schok 3-1A	2.55-2.60	-2.03 - -1.98	extremely silty clay	not applicable				251 ± 7	13.0 ± 0.3	10.9 ± 0.6	45	45 ± 11	1.4	1.4 ± 0.1	n.a.	n.a.

*U-238 activity concentration based on weighted mean of Th-234, Pb-214, Bi-214 activity concentrations. Pb-210 is also determined and used in calculation to determine post Rn-222 contribution.
**Th-232 activity concentration based on weighted mean Ac-228, Pb-212 and Bi-212 activity concentrations.
***'Used' denotes the water and organic content used in calculations of dose rate when results on this sample were used.
****'Sample' denotes use of measurements performed on the the sample of interest. GS stands for gamma spec results.

Table II. OSL dating results (X/Y coordinates: 181315/517896). Samples NCL-7613048–51 are used for gamma-ray spectrometry and not for dating. The OSL ages for the samples NCL-7613046–7 likely indicate the time of burial of the soil by the overlying peat, rather than the time of deposition of the sand itself

NCL code	Sample code	Depth sample (m below surface)	Elevation sample (m Dutch O.D.)	Grainsize for analysis (μm)	Palaeodose (Gy)	Overdispersion (%)	Dose rate (Gy/ka)	Age (ka)	Age (CE/BCE)	Remarks age model used
NCL-7613036	Schok 1-1	0.37-0.39	0.18-0.20	180-212	0.32 ± 0.02	17 ± 4	1.40 ± 0.07	0.23 ± 0.02	1782 ± 21 CE	BSMAM, sigmab 16 ± 4%
NCL-7613037	Schok 1-2	0.44-0.50	0.07-0.13	180-212	0.42 ± 0.03	16 ± 5	2.25 ± 0.13	0.19 ± 0.02	1822 ± 17 CE	BSMAM, sigmab 16 ± 4%
NCL-7613038	Schok 1-3	0.54-0.60	-0.03-0.03	180-212	0.49 ± 0.03	14 ± 4	2.14 ± 0.13	0.23 ± 0.02	1782 ± 20 CE	BSMAM, sigmab 16 ± 4%
NCL-7613039	Schok 1-4	0.64-0.70	-0.13 - -0.07	180-212	0.55 ± 0.03	14 ± 3	2.31 ± 0.15	0.24 ± 0.02	1772 ± 21 CE	BSMAM, sigmab 16 ± 4%
NCL-7613040	Schok 1-5	0.77-0.83	-0.26 - -0.20	90-180	0.64 ± 0.05	61 ± 13	2.41 ± 0.14	0.27 ± 0.03	1742 ± 26 CE	BSMAM, sigmab 13 ± 4%
NCL-7613041	Schok 2-1	1.14-1.16	-0.59 - -0.57	63-90	0.96 ± 0.04	38 ± 5	2.39 ± 0.15	0.40 ± 0.03	1612 ± 30 CE	BSMAM, sigmab 9 ± 4%
NCL-7613042	Schok 2-2	1.16-1.18	-0.61 - -0.59	63-90	0.98 ± 0.03	35 ± 7	2.47 ± 0.17	0.40 ± 0.03	1612 ± 29 CE	BSMAM, sigmab 9 ± 4%
NCL-7613043	Schok 2-3	1.18-1.20	-0.63 - -0.61	63-90	0.88 ± 0.19	20 ± 10	2.48 ± 0.17	0.35 ± 0.08	1662 ± 81 CE	BSMAM, sigmab 9 ± 4%
NCL-7613044	Schok 2-4	1.28-1.30	-0.73 - -0.71	63-90	1.07 ± 0.08	34 ± 10	2.50 ± 0.16	0.43 ± 0.04	1582 ± 41 CE	BSMAM, sigmab 9 ± 4%
NCL-7613045	Schok 2-5	1.30-1.32	-0.75 - -0.73	63-90	0.98 ± 0.15	16 ± 8	2.45 ± 0.15	0.40 ± 0.07	1612 ± 68 CE	BSMAM, sigmab 9 ± 4%
NCL-7613046	Schok 3-1	2.60-2.66	-2.09 - -2.03	212-250	3.84 ± 0.20	13 ± 2	1.10 ± 0.07	3.50 ± 0.30*	1488 ± 291 BCE	BSMAM, sigmab 18 ± 4%
NCL-7613047	Schok 3-2	2.74-2.79	-2.22 - -2.17	212-250	6.53 ± 1.02	35 ± 6	1.30 ± 0.06	5.04 ± 0.82**	3028 ± 818 BCE	BSMAM, sigmab 18 ± 4%

*Age based on younger fraction of grains; reflects final stage of bioturbation rather than depositional age.
**Age unreliable, as it is probably partially affected by bioturbation. Hence it does not adequately reflect the time of bioturbation nor the time of deposition.

~10 ‰ (Murray, 2006), which, combined with high sand (~10–62 vol%) and $CaCO_3$ content (~6 – 10 wt%) and relatively low organic matter content (max. ~4.5 wt%) (Figure 4), point to a marginal marine environment.

Geochronology

The sand of unit 1 has been dated by two OSL dates (Figure 4; Table 2), providing age estimates of 5.0 ± 0.8 and 3.5 ± 0.3 ka. These dates are surprisingly young given the expected Late Pleistocene age (~14.7 – 11.7 ka) for unit 1 (Wiggers, 1955; Spek *et al.*, 1997). As the samples were taken from the palaeosol, and D_e distributions are highly overdispersed, it seems likely that part of the grains were exposed to light due to bioturbation processes after initial deposition. The ages, especially for the upper sample, hence reflect the time when bioturbation at this level ceased due to burial of the deposit (by unit 2), rather than the time of deposition of the sandy deposits. This would imply that the peat sequence (unit 2) started forming after ~1500 ± 300 BCE. The age of the lower sample (~3000 ± 820 BCE) is questionable, as only ~17% of single aliquot estimates agrees with the BSMAM derived burial dose estimate (see Figure 5).

The top of the peat of unit 2 is dated by ^{14}C AMS at 650–690 CE (Table III), indicating the maximum age for the overlying clay (unit 3).

The ten sandy laminae (max. ~2 cm thick) within the clay sequence (unit 3) were dated by OSL (Figure 4; Table II). The lower five samples resulted in ages ranging from 1582 ± 41 to 1662 ± 81 CE. There was no trend of age with depth, and most dates indicate an early 17th century age. A weighted mean of the ages, taking into account shared and unshared errors between samples (Rhodes *et al.*, 2003), indicates that deposition occurred in a relatively short period of time around 1610 ± 26 CE. The upper five OSL samples provided age estimates between 1742 ± 26 and 1822 ± 17 CE. The OSL ages are internally consistent (their ages increase with depth), except for the upper sample (Schok 1-1). Altogether, the OSL ages suggest two distinct periods with high accumulation rates, possibly related to two storm periods.

Discussion

Palaeogeographical development and geochronology unit 3

Following Van den Biggelaar *et al.* (2014), the clay sequence (unit 3) can be divided into three subunits (see Figure 4). From base to top this sequence is partitioned into subunit 3.1 (–123 to –103 cm OD), subunit 3.2 (–103 to –23 cm OD) and subunit 3.3 (–23 to 57 cm OD). Each of these three subunits represent a different environment and are discussed below.

The transition from unit 2 to subunit 3.1 was dated by Van den Biggelaar *et al.* (2014) to 770–940 CE using ^{14}C AMS. In this study the same transition is dated at 650–690 CE (Table III ; Figure 1(B)), also using ^{14}C AMS. The age estimate difference must be due to the different sampling locations. Spatial variations in the age of the top of the peat may be related to slow peat accumulation rates (80 cm in ~2200 years; top 10 cm = ~275 years), peat oxidation by peat-land reclamation and by minor erosion during inundation at the onset of clay deposition. Although the upper surface of the peat unit has some elevation differences across Schokland (Van den Biggelaar *et al.*, 2014), this is most likely due to compaction effects by embankments and the weight of the overlying clay unit 3. As the relief of

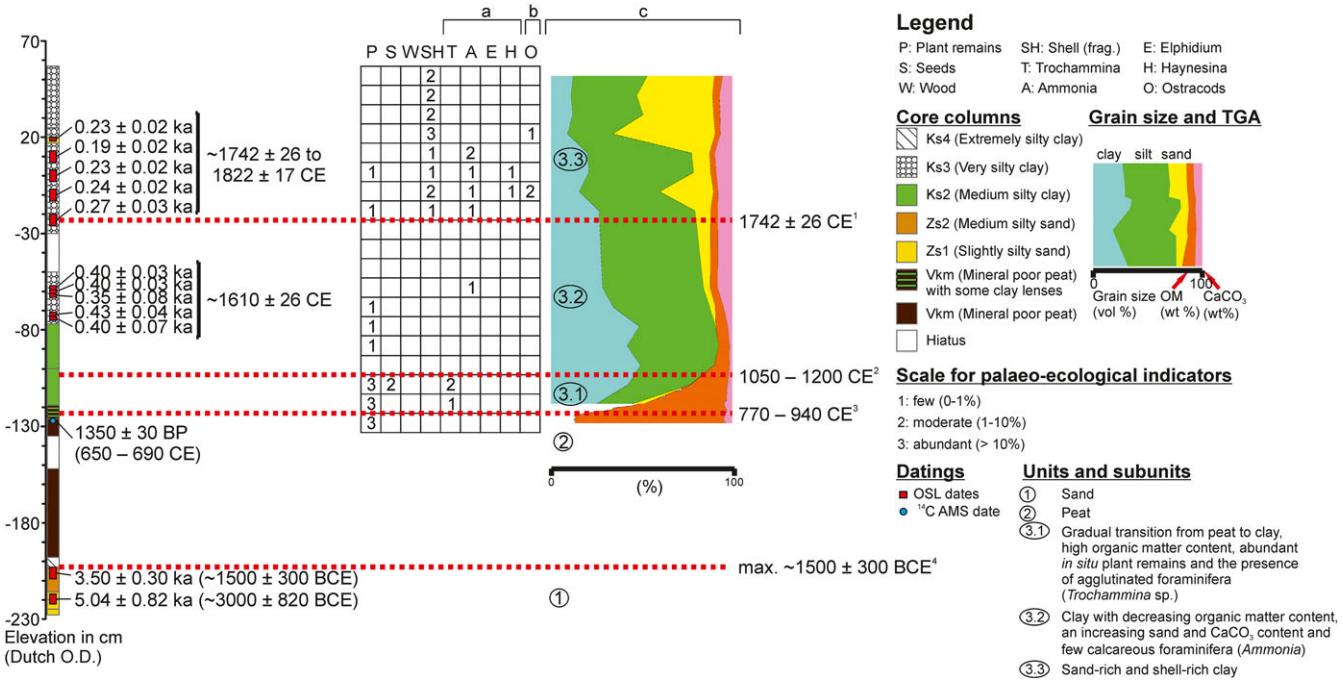

Figure 4. Lithology of coring with grain size, TGA and palaeo-ecological data and dating results (AMS and OSL). Also, the presence of (a) foraminifera, (b) ostracods and (c) a general increase in the sand and CaCO3 content and decrease in the organic matter content from base to top is shown. The differentiation of the lithological units (red lines) is based on Van den Biggelaar *et al.* (2014). The age of the (sub) units is indicated by the black dates: (1) 1742 ± 26 CE, OSL date (this study); (2) 1050–1200 CE, reclamation of the peatlands and construction of embankments (see Van den Biggelaar *et al.*, 2014); (3) 770–940 CE, AMS dates (Van den Biggelaar *et al.*, 2014); (4) max. 1500 ± 300 BCE, OSL date (this study). For location of the core, see Figure 1(B). [Colour figure can be viewed at wileyonlinelibrary.com]

the Pleistocene surface at the former island was levelled by peat growth (Van den Biggelaar *et al.*, 2014), limited spatial variation in the age of the base of unit 3 is expected. Therefore, the date 770–940 CE presented in Van den Biggelaar *et al.* (2014) remains the maximum age of the clay cover (unit 3).

The transition from unit 2 to subunit 3.1 occurred gradually (Van den Biggelaar *et al.*, 2014), representing the transformation of the area from a reed-sedge swamp to an environment that was inundated only occasionally (e.g. during spring tide and storm surges). The inferred low energetic conditions at that time are in agreement with the presence of *in situ* plant remains, arenaceous foraminifer *Trochammina* sp., seeds of *Ranunculus* and a relatively low $CaCO_3$ content. This is consistent with the results from previous research which also indicate weakly brackish conditions at Schokland during the deposition of subunit 3.1 (Van der Heide and Wiggers, 1954; Wiggers, 1955; Van den Biggelaar *et al.*, 2014).

The increased tidal influence that existed at the former island during the deposition of overlying subunit 3.2 is inferred from the increase in sand content, together with the presence of calcareous foraminifers and storm-sand laminae. This is in accordance with the results from previous research which confirm the presence of clay with storm surge sediments, brackish foraminifer species and increasing sand content (Van den Biggelaar *et al.*, 2014). The transition from a weakly brackish (subunit 3.1) to a brackish environment (subunit 3.2) was tentatively correlated to the period 1050–1200 CE using archaeological remains (see Van den Biggelaar *et al.*, 2014). In the present study no age determination for this transition was possible due to the lack of dateable organic and/or sandy material at the lower boundary of subunit 3.2. Therefore the date of 1050–1200 CE for this boundary remains tentative.

The top subunit (3.3) at Schokland is characterized by a marginal marine environment on the basis of the presence of bivalve shell remains, ostracods and the calcareous foraminifer species in that subunit. This is in concordance with the results from previous research which indicate the presence of clay with brackish and marine shells, foraminifers and ostracods at Schokland (Van den Biggelaar *et al.*, 2014) and in the northern part of Flevoland (Noordoostpolder) (Muller and Van Raadshoven, 1947). Apart from these palaeo-ecological indicators, the relatively low organic matter content and high $CaCO_3$ and sand content in the clay are also indicative for a marine influence (see also Van den Biggelaar *et al.*, 2014). The start of the marginal marine environment (subunit 3.3) was tentatively correlated to around 1600 CE by Van den Biggelaar *et al.* (2014), based on historical data indicating the increasing costs for the defense against the sea (e.g. repairs on embankments and loss of land: Resolutie Ridderschap en Steden van Overijssel 1620 and 1629 in Geurts, 1991). Furthermore, sediments with brackish and marine shells, foraminifers and ostracods are present in the Noordoostpolder (Muller and Van Raadshoven, 1947). The maximum age of these sediments was dated to the early 17th century on the basis of shipwrecks (Muller and Van Raadshoven, 1947; Van der Heide and Wiggers, 1954). As these marine sediments are also present on Schokland itself (Van der Heide and Wiggers, 1954), a similar age for these sediments on the former island was expected. However, on the basis of the OSL dates presented in this study (Figure 4), the lower boundary of subunit 3.3 is slightly younger, and is now dated at 1742 ± 26 CE. The surface elevation at the site location was higher than the surrounding region during the 19th century (Mees, 1847). Possibly, during the 17th and 18th centuries the site was also elevated above its surrounding, thereby delaying deposition of marine sediments.

The lack of sedimentary deposits of storm surges that occurred prior to 1600 CE may also be related to elevation of the site location, but firm conclusions on this issue would require additional information from other locations. Another possibility for the age discrepancy of marine sediments between the site location and the surrounding region is that the postulated increase in marine influence around 1600 CE should be

Table III. Two 14C AMS dates of top peat samples (sample Beta-358770: Van den Biggelaar et al., 2014; sample Beta-358771: this study). For location of the core and the samples see Figure 1(B) and (C)

Laboratory no.	X-coord.	Y-coord.	Depth sample (cm below surface)	Elevation sample (cm below Dutch O.D.)	Dated fraction	Age (^{14}C yr BP)	Age (CE/BCE; 2σ)	Remarks
Beta-358770	181263	518830	172-170	427-425	*Betula* periderm, *Pinus*, *Salix* bractae, *Juncus*	1180 ± 30	770-940 CE	14C AMS date top peat of terrestrial plant, seed and wood material. No AAA pre-treatment possible due to insufficient terrestrial organic material (Van den Biggelaar *et al.*, 2014)
Beta-358771	181315	517896	183-185	128-126	*Sphagnum*, *Galium palustre* seed, *Carex* seed, *Alisma* seed, *Betula* periderm, *Epilobium*seed	1350 ± 30	650-690 CE	^{14}C AMS date top peat of terrestrial plant and seed material

situated at –75 cm OD instead at –23 cm OD. This is based on the OSL dates in the present study, combined with the elevation of the lowermost storm-sand laminae, decrease of clay content and increase of sand and $CaCO_3$ content in the clay sequence (Figure 4). However, the near absence of palaeo-ecological indicators indicative for a marine environment in subunit 3.2 at the site location suggests otherwise. To better understand the reason for this age discrepancy we recommend further investigation regarding the preservation potential of these indicators at Schokland.

Correlating storm surge signatures at Schokland to historical storm events

This research shows that storm events dating to the early 17th and 18th to early 19th centuries flooded Schokland. Buisman (2000, 2006, 2015) and Van Malde (2003) published data on storm events that affected the coastal lowlands of the Netherlands during these centuries. According to these data, the two major storm surges that hit the area around the early 17th century occurred in 1610 and 1625 CE. OSL chronology of the sedimentary remains at Schokland that date to 1610 ± 26 CE indicate deposition within a short period, potentially during one or both of these storm surge events.

For the storm surge sediments at the former island that date between 1742 ± 26 and 1822 ± 17 CE, OSL ages suggest deposition over a period of ~80 years. During the 18th and early 19th centuries Schokland was hit by major storm surges in 1775, 1776, 1824 and 1825 CE (Meijlink, 1858; Moerman and Reijers, 1925; Buisman, 2015). The storm surge remains at Schokland that date between 1742 ± 26 and 1822 ± 17 CE could be the result of deposition by several or all of these surges.

However, an alternative interpretation of the sequence, with rapid deposition around 1780 CE, is also possible. In that case, these storm surge deposits could possibly be attributed to either one or both of the 1775 and 1776 CE storm events. Such difficulties in interpreting the data are inherent to uncertainties related to OSL dating; the slight stratigraphic inconsistency in this sequence, indicates the presence of an additional source of error that is not contained in the uncertainty estimates provided in Table II. Although the OSL ages provide a decadal resolution in this age range, robust inferences on deposition during major event(s) or a sequence of minor events would require an even larger data set of samples from the interval of interest.

Interestingly, the light exposure of grains from these deposits shows a clear trend. The lower sample (NCL-7613040) is poorly bleached (overdispersion 61%), while the overlying four samples (NCL7613036-39) are all remarkably well-bleached (with overdispersion 14–17%) (Table II). This implies that for the latter samples, nearly all grains were exposed sufficiently to daylight to have their fast-component OSL signal completely reset. This may suggest reworking of the deposits in several events, or the uptake of near-coastal material by the storm-surges that was exposed to light prior to the storm surge event.

According to Buisman (2000, 2006), major storm surges hit the Zuiderzee area in 1651, 1665 and 1675 CE. The OSL data in this study indicate a lack of storm surge deposits at the site location, present in the northwestern part of Schokland, for the period between 1610 ± 26 and 1742 ± 26 CE. Historical information indicates that, at least until the end of the 18th century, no wooden sea defence was present in the northwestern part of Schokland (Resolutie Staten van Holland 13

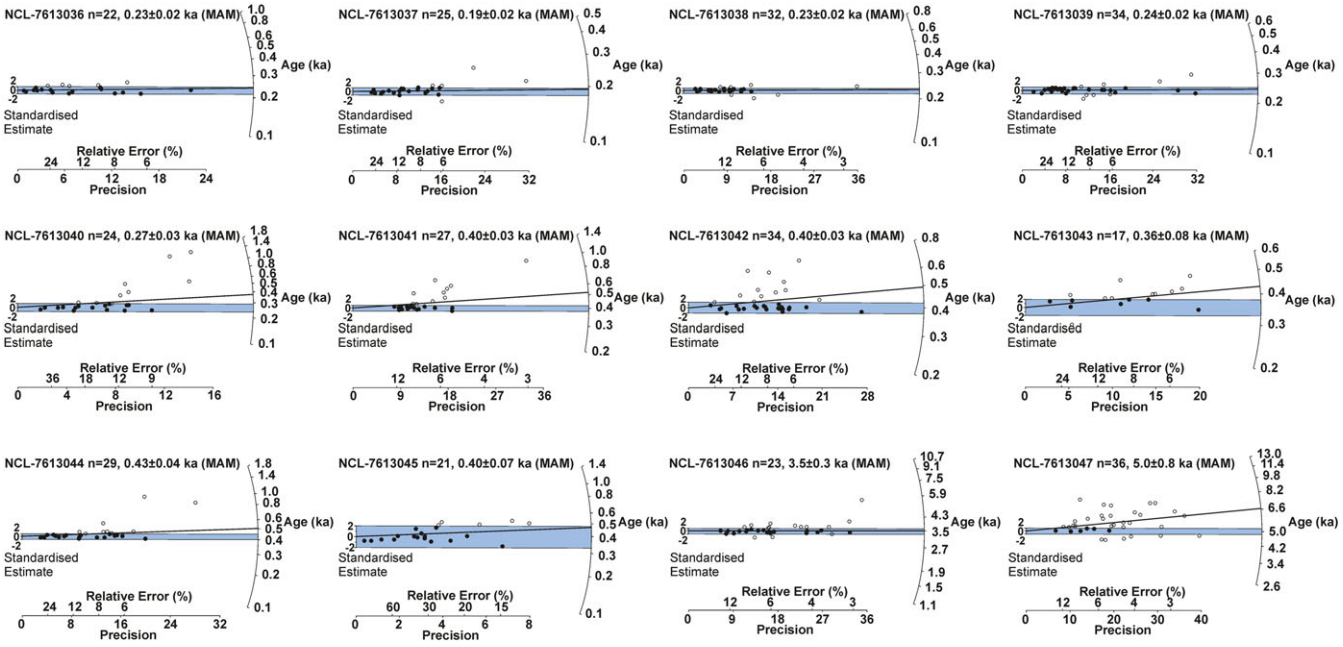

Figure 5. Radial plots (Galbraith, 1990) for each OSL sample, indicating single-aliquot luminescence ages (open and filled dots) and the sample age when applying the bootstrapped MAM (shading: Cunningham and Wallinga, 2012) or the CAM (black solid line: Galbraith *et al*., 1999). These plots are similar to the equivalent dose distributions of each aliquot, because these graphs were constructed by dividing the equivalent dose estimates by the sample dose rate (identical for each aliquot of a sample). The precision used to produce these graphs is based on random uncertainties in equivalent dose only (thus systematic uncertainties in equivalent doses due to beta source calibration as well as dose rate uncertainties are not included). The age estimate is plotted on the curved y-axis and the measurement precision of equivalent dose estimate on the x-axis. Solid dots fall within the final age estimate (shaded area). The percentage of single-aliquot ages within the shaded area indicates the robustness of the estimated age. [Colour figure can be viewed at wileyonlinelibrary.com]

December 1788 in Moerman and Reijers, 1925). This implies that this part of the island must have been vulnerable for storm surges during the period 1610 ± 26 to 1742 ± 26 CE. In addition, the cores and the samples shows no signs of erosion. Altogether, we infer that storm surges flooding the sample site must have occurred within the period 1610 ± 26 to 1742 ± 26 CE. Sediments associated with these events could possibly be represented by the few thin sandy layers present at the site location within subunit 3.2 at an elevation of –51 to –52 cm OD (Figure 1(C)). However, these layers were not sampled for OSL dating as they were mixed with more recent sediments during the coring process and therefore not suitable for OSL dating.

Storm surge impact at Schokland

During the deposition of subunit 3.1, between 770 and 940 CE and 1050–1200 CE, the connectivity between the North Sea and the Flevomeer area increased (Vos and De Vries, 2013). Although storm surges could access the area (e.g. 838 CE storm surge: Buisman, 1995; Gottschalk, 1971), the limited thickness of this subunit (i.e. 20 cm; Figure 4) indicates that there was limited tidal influence at the site location. This is in agreement with the limited thickness of this subunit at other parts of Schokland (max. 88 cm thick; Van den Biggelaar *et al*., 2014).

The reconstructed brackish environment (subunit 3.2) at the former island between 1050 and 1200 CE and 1742 ± 26 CE is in agreement with the counteractive measures that the inhabitants of Schokland took to deal with the impact of the Zuiderzee at that time. These measures consisted of the construction of coastal defences in the area since 1200 CE (Moerman and Reijers, 1925; Van der Heide and Wiggers, 1954; Hogestijn, 1992), migrating to artificially-created higher grounds within the Schokland area (Van der Heide and Wiggers, 1954), changing to a subsistence economy predominantly oriented on fishing from the 15th century onwards (Van der Heide and Wiggers, 1954) and maintaining the wooden sea defence that was present at some parts of Schokland during the 17th and 18th centuries (Resolutie Ridderschap en Steden van Overijssel 1629 in Geurts, 1991; Moerman and Reijers, 1925). Although many of these measures were taken to protect the inhabitants of Schokland against the impact of the Zuiderzee, they could not prevent the large-scale erosion of the former island that occurred between 1200 CE and the end of the 18th century (Figure 3). This increasing impact of the Zuiderzee on Schokland is consistent with the thicker clay cover of subunit 3.2 compared with that of subunit 3.1 (Figure 4; see also Van den Biggelaar *et al*., 2014). At the site location, the major part of the clay of subunit 3.2 was deposited around 1610 ± 26 CE (~50 cm; Figure 4). Possibly, the construction of the wooden sea defence that existed at some parts of Schokland since the early 17th century was initiated as a response to this deposition.

The dominant impact of the Zuiderzee on Schokland during the deposition of subunit 3.3 is in agreement with historical accounts that describe this impact (Mees, 1847; Meijlink, 1858). In addition, to counter the marine influence on Schokland heavy financial investments were made in coastal defences by constructing a stone embankment at the beginning of the 19th century and a stone shore halfway through the 19th century at the western part of the former island (Mees, 1847). The increasing influence on Schokland of the Zuiderzee during the deposition of subunit 3.3 is also reflected by the higher sedimentation rate at the site location at that time (80 cm in 200 years) compared to the period when subunit 3.2 was deposited (80 cm in 550–700 years). The increase in sedimentation rate is in concordance with the general encroachment of the coastline to present-day Schokland (Figure 3; see also Van den Biggelaar *et al*., 2014).

Correlating storm surge signatures at a regional scale

Major storm surges that hit Schokland during the early 17th and 18th to early 19th centuries also had an impact at various other locations along the Dutch coast (Buisman, 2000, 2006, 2015; Van Malde, 2003). Although the Dutch coastline has receded since the Early Medieval Period (Jelgersma *et al.*, 1970), sediments associated with these surges are sometimes preserved in this area (Jelgersma *et al.*, 1995; Cunningham *et al.*, 2011a; Figure 1(A)). Due to this preservation, sedimentary remains of surges in different parts of the coastal areas of the Netherlands that are less than 10 m above sea level (LECZ) can potentially be correlated with each other. Based on chronology, there could be a link between the sandy shell unit near Heemskerk at the Dutch central western coast that was OSL-dated to 1758 ± 15–1780 ± 11 CE by Cunningham *et al.* (2011a) and the shell-bearing sandy layers within subunit 3.3 at Schokland that were dated in this study to 1742 ± 26 to 1822 ± 17 CE (Figures 1(A) and 4). During the second half of the 18th century the Dutch coast was hit by major storm surges in 1775 and 1776 CE (Hering, 1776, 1778). The Heemskerk storm surge deposits have been attributed to the 1775 CE event based on historical sources combined with modelling of storm surge and runup (Cunningham *et al.*, 2011a; Baart *et al.*, 2011). Data published by Buisman (2015) indicates that Schokland was also hit during the 1775 CE storm event. Although sedimentary remains of that event could still be present at Schokland within the sequence that was dated between 1742 ± 26 and 1822 ± 17 CE, this sequence could also be the combined result of deposition by other storm surges. Therefore, the correlation between the 1775 CE storm surge sediments at Heemskerk and Schokland remains tentative.

Currently, it is not possible to link the OSL-dated sedimentary remains of storm surges from the central western coast of the Netherlands and Schokland to other locations within the LECZ of the southern North Sea area due to a lack of data on such remains. As storm surge deposits have a high preservation potential (Kumar and Sanders, 1976), it is most likely that such deposits are still present in some parts of the southern North Sea coast, but they have so far not been found and dated. However, as some of these coastal areas eroded heavily during the 20th century (Reichmüth and Anthony, 2002; Anthony, 2013), and possibly continued to erode since that time, the number of preserved late Holocene storm surge deposits in these areas could decrease rapidly in the future. To establish records of past flood magnitude and frequency in the southern North Sea region, storm surge sediments in areas distant from the coastline that are less affected by present-day marine erosion, such as back-barrier environments, should also be studied. Previous research in the western North Atlantic indicated that such environments contain storm surge sediments that can be used to reconstruct past storm frequency (Donnelly *et al.*, 2001, 2004; Boldt *et al.*, 2010). In these studies a variety of techniques was used for age control of storm surge records, such as ^{14}C AMS dating of interbedded organic material, ^{137}Cs measurements and bulk Pb chronology. Although these techniques provided high resolution flood records, the storm surge sediments themselves were not dated. With the methodology applied in this paper, such sediments can be OSL-dated with a high degree of precision. This precision will likely increase the resolution of storm surge records and thereby also improve insight to flood frequency. In addition, the high resolution OSL dating of storm surge sediments is of paramount importance to link such sediments of similar age at various locations. These links could further improve records of past flood frequency. Apart from frequency, determining the magnitude of past storm events is also of utmost importance for future flood risk assessment. Although information on storm surge magnitude can be obtained from storm surge sediments present in coastal dunes (Baart *et al.*, 2011; Cunningham *et al.*, 2011a), the ability to link these sediments to storm surge deposits of the same age in other landscape settings (e.g. back-barrier environments) could possibly help to improve modelling of the surge and runup that deposited these sediments.

Future Implications

The OSL methodology presented in this paper can be used to assess flood risk in the LECZ by dating past flooding records, allowing to infer storm events and associated floods beyond the period of instrumental records, and matching them to historical data. This has two advantages. First, this extension is crucial to improve modelling of the exceedance frequency of extreme water levels. These levels are used to determine the crest level of flood defences (Maris *et al.*, 1961) and therefore contribute to reduce the probability of flooding. In addition, improved insight to extreme water levels is also important for efficient use of economic resources on flood defence management. Second, with a possible relationship between change in storminess and future climatic conditions (Seneviratne *et al.*, 2012), extension of the data record can be used to better understand this relationship by including storm activity and climatic parameters at centennial to millennial scales. Aside from reducing the probability of flooding, flood risk can also be decreased by limiting flood impact (MVW, 2009). This is illustrated by the Schokland example. While large parts of Schokland flooded during major storm events (Commelin, 1726; Meijlink, 1858), even though embankments were constructed and maintained (Meijlink, 1858; Moerman and Reijers, 1925), these floods had limited impact on the urban areas of the former island as they were built on artificially raised areas. As at Schokland, the combination of reducing the probability of flooding and mitigating flood consequences could be of paramount importance to reduce flood risk in the LECZ under a changing climate.

Apart from matching storm surge deposits to historical data, the state-of-the-art OSL methods applied in this research could possibly also be used to date pre-historical storm surge deposits. Dating such deposits is of major importance to improve modelling of return periods of extreme water levels beyond the period of instrumental and historical records and may help to improve predictions of storminess in a changing climate.

Conclusions

- This study shows that OSL dating can be used to date sedimentary remains that are relatively young, heterogeneous on a millimetre scale and most likely bleached heterogeneously with a high degree of precision.
- The applied OSL methodology is vital to improve records of past flood frequency and magnitude by extending data on storm events beyond the period of instrumental records. Matching these data to historical data on storm events and associated floods can contribute to the assessment of future storm surge risk.
- At Schokland flood risk was reduced by the combined approach of decreasing the probability of flooding (constructing and maintaining embankments) and limiting flood impact (constructing urban areas at raised mounds). Such a combined approach could be of major importance for future coastal management policies under a changing climate.

Acknowledgements—This research was part of the PhD project of Don F.A.M. van den Biggelaar at the Vrije Universiteit Amsterdam (VU). This project, which was successfully finished in February 2017, was part of the multidisciplinary 'Biography of the New Land' research program of CLUE (VU), in collaboration with the Nieuw Land Heritage Centre (Lelystad, The Netherlands). This program is jointly funded by the research institute CLUE (VU) and the Nieuw Land Heritage Centre (Lelystad, The Netherlands). The Netherlands Centre for Luminescence dating (NCL) is supported by the Netherlands organization for scientific research (NWO-ALW; grant #834.03.003). OSL dating of the sediment core from Schokland was funded by the Province of Flevoland.

We thank TNO Geological Survey of the Netherlands (TNO) for providing facilities to separate and store the mechanical coring. Furthermore, we thank Henny Mensink and Jeroen Schokker at TNO for describing the core and an anonymous staff member at TNO for photographing the core.

Facilities for grain size analysis, TGA and palaeo-ecological analysis were provided by the Sediment Laboratory of the Vrije Universiteit Amsterdam. We thank Martin Konert and Martine Hagen (Sediment Laboratory, VU) for their help on these analyses and Ruben Lelivelt (VU) for his support at the fieldwork activity.

References

Aitken MJ. 1985. *Thermoluminescence Dating*. Academic Press: Orlando, FL.

Aitken MJ. 1998. *An Introduction to Optical Dating: The Dating of Quaternary Sediments by the Use of Photon-Stimulated Luminescence*. Oxford University Press: New York.

Anthony EJ. 2013. Storms, shoreface morphodynamics, sand supply, and the accretion and erosion of coastal dune barriers in the southern North Sea. *Geomorphology* **199**: 8–21. https://doi.org/10.1016/j.geomorph.2012.06.007.

Baart F, Bakker M, Van Dongeren A, Den Heijer C, Van Heteren S, Smit M, Van Koningsveld M, Pool A. 2011. Using 18th century storm-surge data from the Dutch Coast to improve the confidence in flood-risk estimates. *Natural Hazards & Earth System Sciences* **11**: 2791–2801. https://doi.org/10.5194/nhess-11-2803-2011.

Blake E, Kimberlain T, Berg R, Cangialosi J, Beven J, II. 2013. *Tropical Cyclone Report: Hurricane Sandy (AL182012), 22– 29 October 2012*. National Hurricane Center: Miami.

Boldt KV, Lane P, Woodruff JD, Donnelly JP. 2010. Calibrating a sedimentary record of overwash from Southeastern New England using modeled historic hurricane surges. *Marine Geology* **275**: 127–139. https://doi.org/10.1016/j.margeo.2010.05.002.

Bosch JHA. 2000. *Standaard Boor Beschrijvingsmethode, versie 5.1*. TNO-NITG: Zwolle.

Buisman J. 1995. *Duizend jaar weer, wind en water in de Lage Landen*. Deel 1: tot 1300. Van Wijnen: Franeker.

Buisman J. 2000. *Duizend jaar weer, wind en water in de Lage Landen*. Deel 4: 1575–1675. Van Wijnen: Franeker.

Buisman J. 2006. *Duizend jaar weer, wind en water in de Lage Landen*. Deel 5: 1675–1750. Van Wijnen: Franeker.

Buisman J. 2015. *Duizend jaar weer, wind en water in de Lage Landen*. Deel 6: 1751–1800. Van Wijnen: Franker.

Buynevich IV, FitzGerald DM, Goble RJ. 2007. A 1500 yr record of North Atlantic storm activity based on optically dated relict beach scarps. *Geology* **35**: 543–546. https://doi.org/10.1130/G23636A.1.

CDC. 2013. Deaths associated with Hurricane Sandy: October-November 2012. *Centers for Disease Control and Prevention: morbidity and mortality weekly report* **62**: 393–397.

Chamberlain E, Wallinga J, Shen Z. in press. Luminescence age modeling of variably-bleached sediment: model selection and input. *Radiation Measurements*. https://doi.org/10.1016/j.radmeas.2018.06.007.

Church JA, Clark PU, Cazenave A, Gregory JM, Jevrejeva S, Levermann A, Merrifield MA, Milne GA, Nerem RS, Nunn PD, Payne A, Pfeffer W, Stammer D, Unnikrishnan A. 2013. Sea level change. In *Climate Change 2013: The Physical Science Basis. Contribution of Working Group I to the Fifth Assessment Report of the Intergovernmental Panel on Climate Change*, Stocker T, Qin D, Plattner G-K, Tignor M, Allen S, Boschung J, Nauels A, Xia Y, Bex V, Midgley P (eds). Cambridge University Press: Cambridge, UK and New York, NY; 1137–1216.

Commelin C. 1726. Beschryvinge van Amsterdam, zynde een naukeurige verhandelinge van desselfs eerste oorspronk uyt den Huyse der heeren van Amstel, en Amstellant, haar vergrooting, rykdom en wyze van regeeringe, tot den Jare 1691/voor dezen uit verscheide oude historie-schryvers by een gesteld, en uitgegeven; en nu uit een meenigte van oude schriften, autentyke stukken en met kopere afbeeldingen verciert, nooit voor desen gedrukt geweest, beschreven en vermeerdert. 2e deel: Amsterdam

Cunningham AC, Bakker MAJ, Van Heteren S, Van der Valk B, Van der Spek AJF, Schaart DR, Wallinga J. 2011a. Extracting storm surge data from coastal dunes for improved assessment of flood risk. *Geology* **39**: 1063–1066. https://doi.org/10.1130/G32244.1.

Cunningham AC, Wallinga J. 2010. Selection of integration time intervals for quartz OSL decay curves. *Quaternary Geochronology* **5**: 657–666. https://doi.org/10.1016/j.quageo.2010.08.004.

Cunningham AC, Wallinga J. 2012. Realizing the potential of fluvial archives using robust OSL chronologies. *Quaternary Geochronology* **12**: 98–106. https://doi.org/10.1016/j.quageo.2012.05.007.

Cunningham AC, Wallinga J, Minderhoud P. 2011b. Expectations of scatter in equivalent-dose distributions when using multi-grain aliquots for OSL dating. *Geochronometria* **38**: 424–431. https://doi.org/10.2478/s13386-011-0048-z.

De Kraker AM. 2002. Historic storms in the North Sea area, an assessment of the storm data, the present position of research and the prospects for future research. In *Climate Development and History in the North Atlantic Realm*, Wefer G, Berger W, Behre KE, Jansen E (eds). Springer-Verlag: Berlin; 415–434.

Donnelly JP, Bryant SS, Butler J, Dowling J, Fan L, Hausmann N, Newby P, Shuman B, Stern J, Westover K. 2001. 700 yr sedimentary record of intense hurricane landfalls in southern New England. *Geological Society of America Bulletin* **113**: 714–727. https://doi.org/10.1130/0016-7606(2001)113<0714:YSROIH>2.0.CO;2.

Donnelly JP, Butler J, Roll S, Wengren M, Webb T. 2004. A backbarrier overwash record of intense storms from Brigantine, New Jersey. *Marine Geology* **210**: 107–121. https://doi.org/10.1016/j.margeo.2004.05.005.

Ente PJ, Koning J, Koopstra R. 1986. De bodem van Oostelijk Flevoland. In *Flevobericht*. Rijksdienst voor de IJsselmeerpolders: Lelystad.

Flather R, Khandker H. 1993. The storm surge problem and possible effects of sea level changes on coastal flooding in the Bay of Bengal. In *Climate and Sea Level Change: Observations, Projections and Implications*, Warrick R, Barrow E, Wigley T (eds). Cambridge University Press: Cambridge; 229–245.

Fruergaard M, Andersen TJ, Johannessen PN, Nielsen LH, Pejrup M. 2013. Major coastal impact induced by a 1000-year storm event. *Scientific Reports* **3**: 1–7. https://doi.org/10.1038/srep01051.

Galbraith RF. 1990. The radial plot: Graphical assessment of spread in ages. *International Journal of Radiation Applications and Instrumentation. Part D. Nuclear Tracks and Radiation Measurements* **17**: 207–214. https://doi.org/10.1016/1359-0189(90)90036-W.

Galbraith RF, Roberts RG, Laslett GM, Yoshida H, Olley JM. 1999. Optical dating of single and multiple grains of quartz from Jinmium rock shelter, northern Australia: Part 1, Experimental design and statistical models. *Archaeometry* **41**: 339–364. https://doi.org/10.1111/j.1475-4754.1999.tb00987.x.

Gerritsen H. 2005. What happened in 1953? The Big Flood in the Netherlands in retrospect. *Philosophical Transactions of the Royal Society A* **363**: 1271–1291. https://doi.org/10.1098/rsta.2005.1568.

Geurts AJ. 1991. Schokland: de historie van een weerbarstig eiland. In *Publikaties van de Stichting voor het bevolkingsonderzoek in de drooggelegde Zuiderzeepolders*. Stichting voor het Bevolkingsonderzoek in de drooggelegde Zuiderzeepolders: Lelystad; 155.

Gottschalk MKE. 1971. *Stormvloeden en rivieroverstromingen in Nederland I, de periode vóór*. Van Gorcum & Comp: Assen; 1400.

Guérin G, Mercier N, Adamiec G. 2011. Dose-rate conversion factors: update. *Ancient TL* **29**: 5–8.

Haigh ID, Wahl T, Rohling EJ, Price RM, Pattiaratchi CB, Calafat FM, Dangendorf S. 2014. Timescales for detecting a significant acceleration in sea level rise. *Nature Communications* **5**: 3635. https://doi.org/10.1038/ncomms4635.

Hering JH. 1776. *Bespiegeling over Neêrlandsch Waternood tusschen den 14den en 15den November 1775*. Loveringh en Allart: Amsterdam.

Hering JH. 1778. *Bespiegeling over Neêrlandsch Waternood tusschen den 21sten en 22sten November 1776*. Johannes Allart: Amsterdam.

Hogestijn JWH. 1992. Schokland in de late Middeleeuwen. In *Schokland Revisited*, Tiesinga GHL (ed). Walburg Pers: Zutphen; 95–112.

Jelgersma S, De Jong J, Zagwijn W, Van Regteren Altena J. 1970. The coastal dunes of the western Netherlands; geology, vegetational history and archeology. *Mededelingen Rijks Geologische Dienst Nieuwe Serie* **21**: 93–167.

Jelgersma S, Stive MJF, van der Valk L. 1995. Holocene storm surge signatures in the coastal dunes of the western Netherlands. *Marine Geology* **125**: 95–110. https://doi.org/10.1016/0025-3227(95)00061-3.

Kates RW, Colten CE, Laska S, Leatherman SP. 2006. Reconstruction of New Orleans after Hurricane Katrina: a research perspective. *Proceedings of the National Academy of Sciences* **103**: 14653–14660. https://doi.org/10.1073/pnas.0605726103.

Klijn F, De Grave P. 2008. Grenzen aan de gevolgen van een overstroming? Een reflectie op de uitkomsten van de Compartimenteringstudie. In *Deltares*.

Kolen B, Slomp R, Van Balen W, Terpstra T, Bottema M, Nieuwenhuis S. 2010. *Learning from French experiences with storm Xynthia; damages after a flood*. HKV consultants and Ministry of Transport, Public Works and Water Management, Centre for Water Management, Rijkswaterstaat, Lelystad.

Kumar N, Sanders JE. 1976. Characteristics of shoreface storm deposits: modern and ancient examples. *Journal of Sedimentary Research* **46**: 145–162. https://doi.org/10.1306/212F6EDD-2B24-11D7-8648000102C1865D.

Lowe JA, Woodworth PL, Knutson T, McDonald RE, McInnes KL, Woth K, Von Storch H, Wolf J, Swail V, Bernier NB, Gulev S, Horsburgh K, Unnikrishnan A, Hunter J, Weisse R. 2010. Past and future changes in extreme sea levels and waves. In *Understanding Sea-Level Rise and Variability*, Church J, Woodworth PL, Aarup T, Wilson W (eds). Wiley-Blackwell: Oxford, UK; 326–375.

Madsen AT, Murray A, Andersen T, Pejrup M, Breuning-Madsen H. 2005. Optically stimulated luminescence dating of young estuarine sediments: a comparison with 210Pb and 137Cs dating. *Marine Geology* **214**: 251–268. https://doi.org/10.1016/j.margeo.2004.10.034.

Maris A, De Blocq van Kuffeler V, Harmsen W, Jansen P, Nijhoff G, Thijssen J, Verloren van Themaat R, De Vries J, Van der Wal L. 1961. *Rapport Deltacommissie. Deel 1. Eindverslag en interimadviezen*. Den Haag: Staatsdrukkerij.

McGranahan G, Balk D, Anderson B. 2007. The rising tide: assessing the risks of climate change and human settlements in low elevation coastal zones. *Environment and Urbanization* **19**: 17–37. https://doi.org/10.1177/0956247807076960.

Mees G. 1847. Schokland. In *Overijsselsche almanak voor oudheid en letterkunde*. J. de Lange: Deventer; 267–330.

Meijlink B. 1858. *Beschrijving van Schokland en de Schokkers, met eenige losse gedachten en gesprekken op een zondags-reisje her en derwaarts*. K. Van Hulst: Kampen.

Mejdahl V. 1979. Thermoluminescence dating: beta-dose attenuation in quartz grains. *Archaeometry* **21**: 61–72. https://doi.org/10.1111/j.1475-4754.1979.tb00241.x.

Menéndez M, Woodworth PL. 2010. Changes in extreme high water levels based on a quasi-global tide-gauge data set. *Journal of Geophysical Research: Oceans* **115**: C10011. https://doi.org/10.1029/2009JC005997.

Moerman HJ, Reijers AJ. 1925. Schokland. *Tijdschrift Koninklijk Nederlands Aardrijkskundig Genootschap*, 2e serie **42**: 151–188.

Mook WG, Streurman. 1983. Physical and chemical aspects of radiocarbon dating. *PACT* **8**: 31–55.

Muis S, Verlaan M, Winsemius HC, Aerts JC, Ward PJ. 2016. A global reanalysis of storm surges and extreme sea levels. *Nature Communications* **7**: 1–11. https://doi.org/10.1038/ncomms11969.

Muller J, Van Raadshoven B. 1947. Het Holoceen in de Noordoostpolder. *Tijdschrift Koninklijk Nederlands Aardrijkskundig Genootschap, 2e serie* **64**: 153–185.

Murray AS, Wintle AG. 2003. The single aliquot regenerative dose protocol: potential for improvements in reliability. *Radiation Measurements* **37**: 377–381. https://doi.org/10.1016/S1350-4487(03)00053-2.

Murray JW. 2006. *Ecology and Applications of Benthic Foraminifera*. Cambridge University Press: New York.

MVW. 2009. *Nationaal Waterplan 2009–2015*. Ministerie van Verkeer en Waterstaat, Ministerie van Volkshuisvesting, Ruimtelijke Ordening en Milieubeheer en het Ministerie van Landbouw, Natuur en Voedselkwaliteit: Den Haag.

Neumann B, Vafeidis AT, Zimmermann J, Nicholls RJ. 2015. Future coastal population growth and exposure to sea-level rise and coastal flooding-a global assessment. *PloS one* **10**: e0118571. https://doi.org/10.1371/journal.pone.0118571.

Oele E, Apon W, Fischer M, Hoogendoorn R, Mesdag C, De Mulder E, Overzee B, Sesören A, Westerhoff W. 1983. Surveying the Netherlands: sampling techniques, maps and their application. *Geologie en Mijnbouw* **62**: 355–372.

Peiffer E. 2017. Still learning: What Hurricanes Harvey and Irma reveal about US disaster policy. Available at: https://www.urban.org, accessed on 20-09-2017.

Prescott JR, Hutton JT. 1994. Cosmic ray contributions to dose rates for luminescence and ESR dating: large depths and long-term time variations. *Radiation Measurements* **23**: 497–500. https://doi.org/10.1016/1350-4487(94)90086-8.

Rappaport E. 2014. Fatalities in the United States from Atlantic tropical cyclones: new data and interpretation. *Bulletin American Meteorological Society* **95**: 341–346. https://doi.org/10.1175/BAMS-D-12-00074.1.

Reichmüth B, Anthony EJ. 2002. The variability of ridge and runnel beach morphology: examples from northern France. *Journal of Coastal Research* (s (36): 612–621. https://doi.org/10.2112/1551-5036-36.sp1.612.

Reimer PJ, Baillie MGL, Bard E, Bayliss A, Beck JW, Blackwell PG, Bronk Ramsey C, Buck CE, Burr GS, Edwards RL, Friedrich M, Grootes PM, Guilderson TP, Hajdas I, Heaton TJ, Hogg AG, Hughen KA, Kaiser KF, Kromer B, McCormac FG, Manning SW, Reimer RW, Richards DA, Southon JR, Talamo S, Turney CSM, Van der Plicht J, Weyhenmeyer CE. 2009. IntCal09 and Marine09 radiocarbon age calibration curves, 0-50,000 years cal BP. *Radiocarbon* **51**: 1111–1150. https://doi.org/10.1017/S0033822200034202.

Rhodes E, Ramsey CB, Outram Z, Batt C, Willis L, Dockrill S, Bond J. 2003. Bayesian methods applied to the interpretation of multiple OSL dates: high precision sediment ages from Old Scatness Broch excavations, Shetland Isles. *Quaternary Science Reviews* **22**: 1231–1244. https://doi.org/10.1016/S0277-3791(03)00046-5.

Rijkswaterstaat KNMI. 1961. Verslag over de stormvloed van 1953. *Staatsdrukkerij en uitgeverijbedrijf: 's Gravenhage*: 714.

Seneviratne SI, Nicholls N, Easterling D, Goodess CM, Kanae S, Kossin J, Luo Y, Marengo J, McInnes K, Rahimi M, Reichstein M, Sorteberg A, Vera C, Zhang X. 2012. Changes in climate extremes and their impacts on the natural physical environment. In *Managing the Risks of Extreme Events and Disasters to Advance Climate Change Adaptation*, Field C, Barros V, Stocker T, Qin D, Dokken D, Ebi K, Mastrandrea M, Mach K, Plattner G-K, Allen S, Tignor M, Midgley P (eds). Cambridge University Press: Cambridge, UK and New York, NY, USA; 109–230.

Spek T, Bisdom EBA, Van Smeerdijk DG. 1997. *Verdronken dekzandgronden in Zuidelijk Flevoland (archeologische opgraving 'A27-Hoge Vaart'): een interdisciplinaire studie naar de veranderingen van bodem en landschap in het Mesolithicum en Vroeg-Neolithicum*. SC-DLO (Rapport/DLO-Staring Centrum 472.1): Wageningen; 187.

Steers J. 1953. The East Coast Floods. *The Geographical Journal* **119**: 280–295. https://doi.org/10.2307/1790640.

Talma AS, Vogel JC. 1993. A simplified approach to calibrating C14 dates. *Radiocarbon* **35**: 317–322. https://doi.org/10.1017/S0033822200014077.

Van den Biggelaar DFAM, Kluiving SJ, Van Balen RT, Kasse C, Troelstra SR, Prins MA. 2014. Storms in a lagoon: flooding history during the last 1200 years derived from geological and historical archives of Schokland (Noordoostpolder, The Netherlands). *Netherlands Journal of Geosciences* **93**: 175–196. https://doi.org/10.1017/njg.2014.14.

Van den Brink H, Können G, Opsteegh J. 2005. Uncertainties in extreme surge level estimates from observational records. *Philosophical*

Transactions of the Royal Society of London A: Mathematical, Physical and Engineering Sciences **363**: 1377–1386. https://doi.org/10.1098/rsta.2005.1573.

Van der Heide GD. 1963. Over het onderhoud van alle de zeewerken op het eiland Schokland. In *Kamper Almanak 1963-1964*, Fehrmann C (ed). Nutsspaarbank: Kampen; 179–200.

Van der Heide GD, Wiggers AJ. 1954. Enkele resultaten van het geologische en archeologische onderzoek betreffende het eiland Schokland en zijn naaste omgeving. In *Langs gewonnen velden (facetten van Smedings werk)*, Zuur AJ (ed). Veenman & Zonen: Wageningen; 96–113.

Van der Wal L. 1923. Geschiedenis van de Plannen tot Afsluiting en Droogmaking van de Zuider Zee, met chronologische lijst van geschriften tot en met het jaar 1922. In *Rapporten en Mededeelingen betreffende de Zuider Zeewerken*: Den Haag.

Van Malde J. 2003. Historische Stormvloedstanden. Aqua Systems International (rapport 2003.08.1). Rijkswaterstaat, Rijksinstituut voor Kust en Zee/RIKZ 138.

Van Vliet-Lanoë B, Goslin J, Hallégouët B, Hénaff A, Delacourt C, Fernane A, Franzetti M, Le Cornec E, Le Roy P, Penaud A. 2014. Middle-to late-Holocene storminess in Brittany (NW France): Part I–morphological impact and stratigraphical record. *The Holocene* **24**: 413–433. https://doi.org/10.1177/0959683613519687.

Vos P, De Vries S. 2013.2^{e} generatie palaeogeografische kaarten van Nederland (versie 2.0). Deltares: Utrecht. Data last retrieved on 14-03-2016 from www.archeologieinnederland.nl.

Wallinga J, Bos IJ. 2010. Optical dating of fluvio-deltaic clastic lake-fill sediments. A feasibility study in the Holocene Rhine delta (western Netherlands). *Quaternary Geochronology* **5**: 602–610. https://doi.org/10.1016/j.quageo.2009.11.001.

Waverley JA. 1954. *Report of the Departmental Committee on Coastal Flooding*. Her Majesty's Stationary Office (British Command Paper 9165): London.

Wiggers AJ. 1955. *De wording van het Noordoostpoldergebied*. University of Amsterdam: Amsterdam; 216.

Wintour P. 2017. Theresa May urged to explain lacklustre Hurricane Irma response. Available at: https://www.theguardian.com, accessed on 20-09-2017.

Worland J. 2017. Why We Won't Be Ready for the Next Hurricane Harvey Either. Available at: http://time.com, accessed on 18-09-2017.

Zuiderzee-vereeniging. 1916. *De watervloed van 13-14 januari 1916*. Brill: Leiden.